Supplement of

Highly oxygenated organic molecules (HOM) formation in the isoprene oxidation by NO_3 radical

Defeng Zhao[1,2], Iida Pullinen[2, a], Hendrik Fuchs[2], Stephanie Schrade[2], Rongrong Wu[2], Ismail-Hakki Acir[2, b], Ralf Tillmann[2], Franz Rohrer[2], Jürgen Wildt[2], Yindong Guo[1], Astrid Kiendler-Scharr[2], Andreas Wahner[2], Sungah Kang[2], Luc Vereecken[2], Thomas F. Mentel[2]

[1]Department of Atmospheric and Oceanic Sciences & Institute of Atmospheric Sciences, Fudan University, 200438, Shanghai, China;
[2]Institute of Energy and Climate Research, IEK-8: Troposphere, Forschungszentrum Jülich, 52425, Jülich, Germany
[a]Now at: Department of Applied Physics, University of Eastern Finland, Kuopio, 7021, Finland.
[b]Now at: Institute of Nutrition and Food Sciences, University of Bonn, Bonn, 53115, Germany;

Correspondence to: Thomas F. Mentel (t.mentel@fz-juelich.de)

In the supplement we describe the derivation of calibration coefficient of NO_3^--CIMS for H_2SO_4. In addition, more tables and figures besides those in the main text are provided.

1 S1 Deriving calibration coefficient of H_2SO_4 in NO_3^--CIMS and HOM yield

In order to convert peak intensity in mass spectra to concentration, the calibration coefficient of H_2SO_4 is derived. H_2SO_4 was produced in-situ in SAPHIR chamber by the oxidation SO $_2$ by OH. SO_2 (~15 ppb) was added into the chamber and the roof was opened to initiate photo-oxidation. In SAPHIR chamber, OH radicals are mainly formed by the photolysis of HONO (nitrous acid) directly coming off the chamber walls through a photolytic process (Rohrer et al., 2005;Zhao et al., 2016). NO (~20 ppb) was added which can enhance OH production by photochemical recycling. OH concentration was characterized by using laser induced fluorescence (LIF) with the details described in (Fuchs et al., 2012). SO_2 concentrations was characterized using an SO_2 analyzer (Thermo Systems 43i).

The concentration of H_2SO_4 in the chamber can be described by the following equation.

$$\frac{d[H_2SO_4]}{dt} = k[SO_2][OH] - (k_{wl} + k_{dil})[H_2SO_4]) \quad \text{(Eq. 1)}$$

where $[H_2SO_4]$, $[SO_2]$, [OH] are the concentration of these species, k is the rate constant for the reaction of SO_2 with OH, k_{wl} is the wall loss rate of H_2SO_4 (~6.0×10^{-4} s^{-1} as characterized for low volatility compounds in our previous publication (Zhao et al., 2018)) and k_{dil} is the dilution rate of H_2SO_4 (~1×10^{-5} s^{-1}).

$$[H_2SO_4]=C\times I \quad \text{(Eq. 2)}$$

where C is the calibration coefficient of H_2SO_4, I is the peak intensity of H_2SO_4 determined by normalized peak area of H_2SO_4 at time t, i.e., the peak area divided by total signal of mass spectrum (termed as normalized count (nc)).

Substituting Eq.2 to Eq. 1, one can get

$$C\frac{dI}{dt} = k[SO_2][OH] - C(k_{wl} + k_{dil})I \quad \text{(Eq. 3)}$$

Integrating Eq.3, one can get

$$C = \frac{k[SO_2][OH]}{\frac{I-I_0}{t}+(k_{wl}+k_{dil})I} \quad \text{(Eq. 4)}$$

where I_0 is the peak intensity at time zero. C was determined to be 2.5×10^{10} molecules cm^{-3} nc^{-1}. The second term of denominator in Eq. 4 is much lower the first term and can omitted. The uncertainty of C was estimated to -52%/+ 101% from the uncertainty of SO_2 concentration (~7 %), OH concentration (~ 10 %), I (~ 10%) and k (Δlogk=±0.3) using error propagation, which corresponds to $(1.2\text{-}5.0)\times10^{10}$ molecules cm^{-3} nc^{-1}. The C value is generally consistent with the value of 3.7×10^{10} molecules cm^{-3} nc^{-1} in our previous calibration (Pullinen et al., 2020).

HOM yield was calculated as

$$Y = \frac{[HOM]}{[VOC]_r} = \frac{I(HOM)C}{[VOC]_r} \quad \text{(Eq. 5)}$$

where [HOM] is concentration of HOM and $[VOC]_r$ is the concentration of VOC reacted. The uncertainty of HOM yield was estimated to -55%/+ 103% from the uncertainty of HOM intensity (~10 %), VOC concentration (~ 15 %) and C using error propagation.

2 S2 Detailed mechanisms of trimer formation

The $C_{15}H_{25}N_5O_n$ series can be formed by the following reactions:

$$C_{10}H_{16}N_3O_{n1}\bullet + C_5H_9N_2O_{n2}\bullet \rightarrow C_{15}H_{25}N_5O_{n1+n2-2} + O_2 \quad \text{RS1}$$

$$C_{10}H_{17}N_4O_{n1}\bullet + C_5H_8NO_{n2}\bullet \rightarrow C_{15}H_{25}N_5O_{n1+n2-2} + O_2 \quad \text{RS2}$$

$$C_{10}H_{18}N_3O_{n1}\bullet + C_5H_7N_2O_{n2}\bullet \rightarrow C_{15}H_{25}N_5O_{n1+n2-2} + O_2 \quad \text{RS3}$$

The $C_{10}H_{18}N_3O_n$ (n=14-20) and $C_{10}H_{17}N_4O_n$ can be formed by the dimers with NO_3.

$$C_{10}H_{18}N_2O_n + NO_3 + O_2 \rightarrow C_{10}H_{18}N_3O_n\bullet \quad \text{RS4}$$

$$C_{10}H_{17}N_3O_n + NO_3 + O_2 \rightarrow C_{10}H_{17}N_4O_n \quad \text{RS5}$$

R21 is likely to be unimportant because both the abundance of $C_{10}H_{18}N_3O_n$ and $C_5H_7N_2O_n$ were low. Since the peaks of $C_{10}H_{18}N_3O_n$ (n=14-20) series overlap with $C_{10}H_{16}N_2O_n$, we can only assign them with low confidence. Similarly, $C_{10}H_{17}N_4O_n$ series overlap with $C_{10}H_{15}N_3O_n$ series (dimer 5).

The $C_{15}H_{25}N_3O_n$ series can be formed by the following reactions:

$$C_{10}H_{17}N_2O_{n1}\bullet + C_5H_8NO_{n2}\bullet \rightarrow C_{15}H_{25}N_3O_{n1+n2-2} + O_2 \quad \text{RS6}$$

$$C_{10}H_{16}NO_{n1}\bullet + C_5H_9N_2O_{n2}\bullet \rightarrow C_{15}H_{25}N_3O_{n1+n2-2} + O_2 \quad \text{RS7}$$

The $C_{15}H_{26}N_4O_n$ series can be formed by the following reactions:

$$C_{10}H_{17}N_2O_{n1}\bullet + C_5H_9N_2O_{n2}\bullet \rightarrow C_{15}H_{26}N_4O_{n1+n2-2} + O_2 \quad \text{RS8}$$

$$C_{10}H_{18}N_3O_{n1}\bullet + C_5H_8NO_{n2}\bullet \rightarrow C_{15}H_{26}N_4O_{n1+n2-2} + O_2 \quad \text{RS9}$$

$$C_{10}H_{16}N_3O_{n1}\bullet + C_5H_{10}NO_{n2}\bullet \rightarrow C_{15}H_{26}N_4O_{n1+n2-2} + O_2 \quad \text{RS10}$$

R28 is likely to be unimportant because both the abundance of $C_{10}H_{16}N_3O_n$ and $C_5H_{10}NO_n$ were low.

The $C_{15}H_{24}N_2O_n$ series can be formed by the following reactions:

$$C_{10}H_{16}NO_{n1}\bullet + C_5H_8NO_{n2}\bullet \rightarrow C_{15}H_{24}N_2O_{n1+n2-2} + O_2 \quad \text{RS11}$$

$C_{10}H_{16}NO_{n1}\bullet$ is formed via R15 as mentioned above.

References:

Fuchs, H., Dorn, H. P., Bachner, M., Bohn, B., Brauers, T., Gomm, S., Hofzumahaus, A., Holland, F., Nehr, S., Rohrer, F., Tillmann, R., and Wahner, A.: Comparison of OH concentration measurements by DOAS and LIF during SAPHIR chamber experiments at high OH reactivity and low NO concentration, Atmos. Meas. Tech., 5, 1611-1626, 10.5194/amt-5-1611-2012, 2012.

Pullinen, I., Schmitt, S., Kang, S., Sarrafzadeh, M., Schlag, P., Andres, S., Kleist, E., Mentel, T. F., Rohrer, F., Springer, M., Tillmann, R., Wildt, J., Wu, C., Zhao, D., Wahner, A., and Kiendler-Scharr, A.: Impact of NOx on secondary organic aerosol (SOA) formation from α-pinene and β-pinene photo-oxidation: the role of highly oxygenated organic nitrates, Atmos. Chem. Phys. Discuss., 2020, 1-40, 10.5194/acp-2019-1168, 2020.

Rohrer, F., Bohn, B., Brauers, T., Bruning, D., Johnen, F. J., Wahner, A., and Kleffmann, J.: Characterisation of the photolytic HONO-source in the atmosphere simulation chamber SAPHIR, Atmos. Chem. Phys., 5, 2189-2201, 2005.

Zhao, D. F., Buchholz, A., Kortner, B., Schlag, P., Rubach, F., Fuchs, H., Kiendler-Scharr, A., Tillmann, R., Wahner, A., Watne, Å. K., Hallquist, M., Flores, J. M., Rudich, Y., Kristensen, K., Hansen, A. M. K., Glasius, M., Kourtchev, I., Kalberer, M., and Mentel, T. F.: Cloud condensation nuclei activity, droplet growth kinetics, and hygroscopicity of biogenic and anthropogenic secondary organic aerosol (SOA), Atmos. Chem. Phys., 16, 1105-1121, 10.5194/acp-16-1105-2016, 2016.

Zhao, D. F., Schmitt, S. H., Wang, M. J., Acir, I. H., Tillmann, R., Tan, Z. F., Novelli, A., Fuchs, H., Pullinen, I., Wegener, R., Rohrer, F., Wildt, J., Kiendler-Scharr, A., Wahner, A., and Mentel, T. F.: Effects of NOx and SO2 on the secondary organic aerosol formation from photooxidation of alpha-pinene and limonene, Atmos. Chem. Phys., 18, 1611-1628, 10.5194/acp-18-1611-2018, 2018.

Supplement figures and tables

$$C_5H_8 \xrightarrow[O_2]{NO_3} C_5H_8NO_5\bullet \xrightarrow[O_2]{H\text{-shift}} C_5H_7NO_4 \xrightarrow[O_2]{OH} C_5H_8NO_7\bullet \xrightarrow{HO_2} C_5H_9NO_7$$

(a)

$$C_5H_8 \xrightarrow[O_2]{NO_3} C_5H_8NO_5\bullet \xrightarrow{RO_2/NO_3} C_5H_8NO_4\bullet \xrightarrow[-NO_2]{H\text{-shift}} C_5H_8O_2 \xrightarrow[O_2]{NO_3} C_5H_8NO_7\bullet \xrightarrow{HO_2} C_5H_9NO_7$$

(b)

Scheme S1. The pathway to form second-generation $C_5H_9NO_7$

$$C_5H_8 \xrightarrow[O_2]{NO_3} C_5H_8NO_5\bullet \xrightarrow[O_2]{H\text{-shift}} C_5H_7NO_4 \xrightarrow[O_2]{OH} C_5H_8NO_7\bullet \xrightarrow{RO_2} C_5H_9NO_6$$

(a)

$$C_5H_8 \xrightarrow[O_2]{NO_3} C_5H_8NO_5\bullet \xrightarrow{RO_2/NO_3} C_5H_8NO_4\bullet \xrightarrow[-NO_2]{H\text{-shift}} C_5H_8O_2 \xrightarrow[O_2]{NO_3} C_5H_8NO_7\bullet \xrightarrow{RO_2} C_5H_9NO_6$$

(b)

Scheme S2. The pathway to form second-generation $C_5H_9NO_6$.

$$C_5H_8 \xrightarrow{NO_3} C_5H_8NO_5\bullet \xrightarrow{H\text{-shift}} C_5H_7NO_4 \xrightarrow{OH} C_5H_8NO_7\bullet \xrightarrow{H\text{-shift}} C_5H_8NO_9\bullet \xrightarrow{HO_2} C_5H_9NO_9$$

(a)

$$C_5H_8 \xrightarrow[O_2]{NO_3} C_5H_8NO_5\bullet \xrightarrow{RO_2/NO_3} C_5H_8NO_4\bullet \xrightarrow[-NO_2]{H\text{-shift}} C_5H_8O_2 \xrightarrow[O_2]{NO_3} C_5H_8NO_7\bullet \xrightarrow[O_2]{H\text{-shift}} C_5H_8NO_9\bullet \xrightarrow{HO_2} C_5H_9NO_9$$

(b)

$$C_5H_8 \xrightarrow[O_2]{NO_3} C_5H_8NO_5\bullet \xrightarrow[O_2]{H\text{-shift}} C_5H_7NO_4 \xrightarrow[O_2]{OH} C_5H_8NO_7\bullet \xrightarrow[O_2]{H\text{-shift}} \xrightarrow[O_2]{H\text{-shift}} C_5H_8NO_{11}\bullet \xrightarrow{RO_2/NO_3} C_5H_8NO_{10}\bullet \xrightarrow{RO_2} C_5H_9NO_9$$

(c)

$$C_5H_8 \xrightarrow[O_2]{NO_3} C_5H_8NO_5\bullet \xrightarrow{RO_2/NO_3} C_5H_8NO_4\bullet \xrightarrow[-NO_2]{H\text{-shift}} C_5H_8O_2 \xrightarrow[O_2]{NO_3} C_5H_8NO_7\bullet \xrightarrow[O_2]{H\text{-shift}} \xrightarrow[O_2]{H\text{-shift}} C_5H_8NO_{11}\bullet \xrightarrow{RO_2/NO_3} C_5H_8NO_{10}\bullet \xrightarrow{RO_2} C_5H_9NO_9$$

(d)

Scheme S3. The pathway to form second-generation $C_5H_9NO_9$.

$$C_5H_8 \xrightarrow[O_2]{NO_3} C_5H_8NO_5\bullet \xrightarrow[O_2]{H\text{-shift}} C_5H_7NO_4 \xrightarrow[O_2]{OH} C_5H_8NO_7\bullet \xrightarrow[O_2]{H\text{-shift}} \xrightarrow[O_2]{H\text{-shift}} C_5H_8NO_{11}\bullet \xrightarrow{RO_2} C_5H_9NO_{10}$$

(a)

$$C_5H_8 \xrightarrow[O_2]{NO_3} C_5H_8NO_5\bullet \xrightarrow{RO_2/NO_3} C_5H_8NO_4\bullet \xrightarrow[-NO_2]{H\text{-shift}} C_5H_8O_2 \xrightarrow[O_2]{NO_3} C_5H_8NO_7\bullet \xrightarrow[O_2]{H\text{-shift}} \xrightarrow[O_2]{H\text{-shift}} C_5H_8NO_{11}\bullet \xrightarrow{RO_2} C_5H_9NO_{10}$$

(b)

Scheme S4. The pathway to form second-generation $C_5H_9NO_{10}$

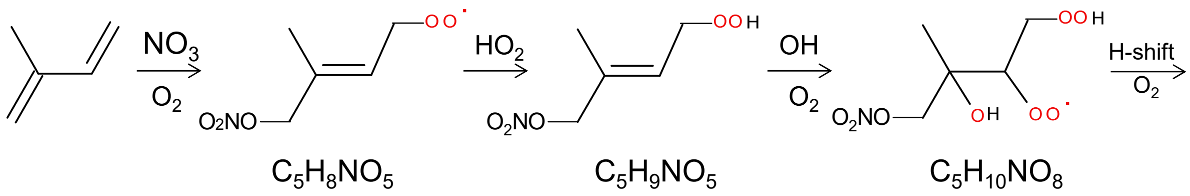

(a)

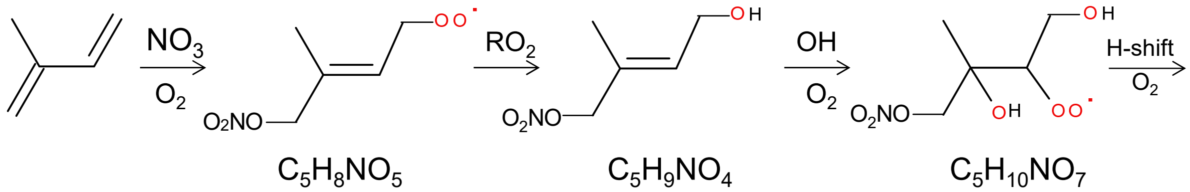

(b)

Scheme S5. The pathway to form $C_5H_{10}NO_{n(n\geq7)}$• RO_2 series with even (a) and odd (b) number of oxygen atoms.

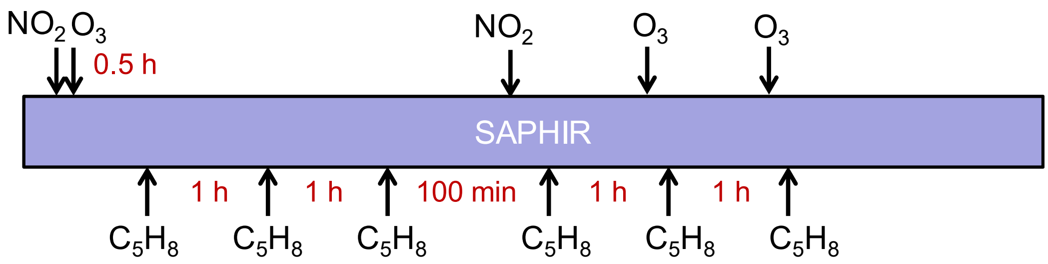

Figure S1. Schematic of the experimental procedure.

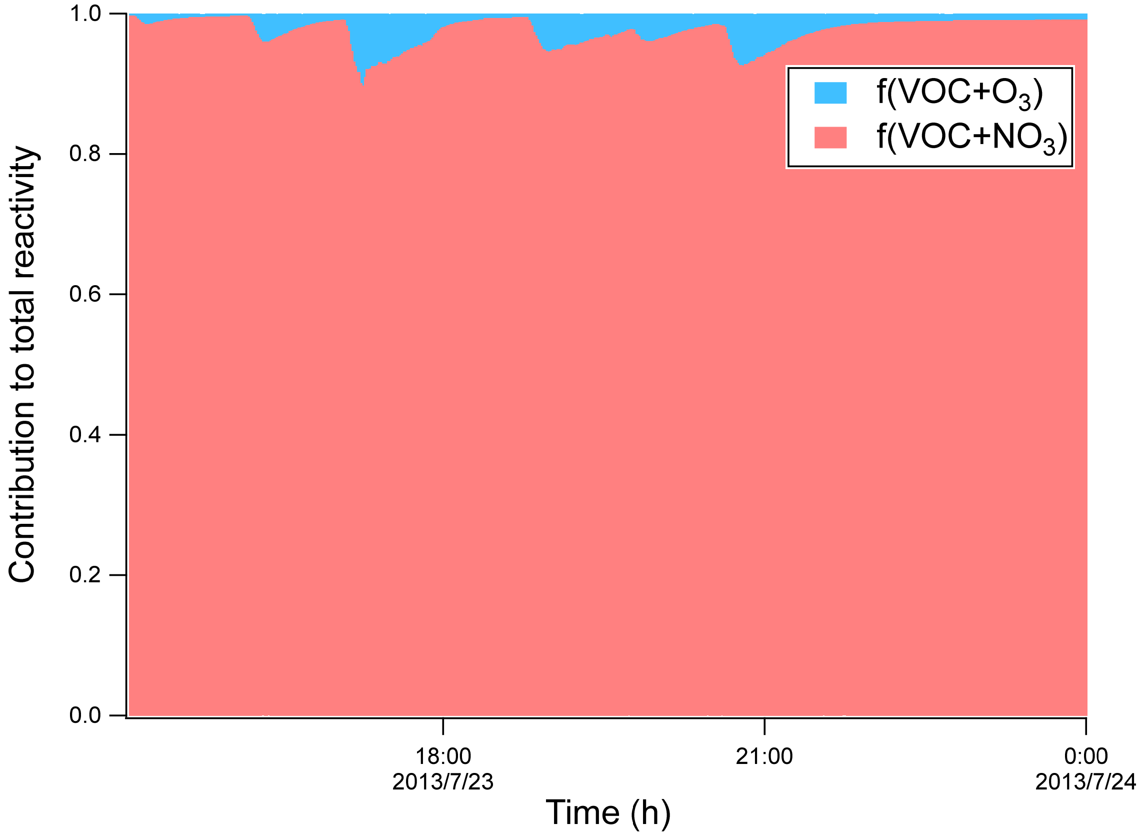

Figure S2. Relative contributions of the reaction rates of isoprene with NO_3 and with O_3 to the total isoprene loss.

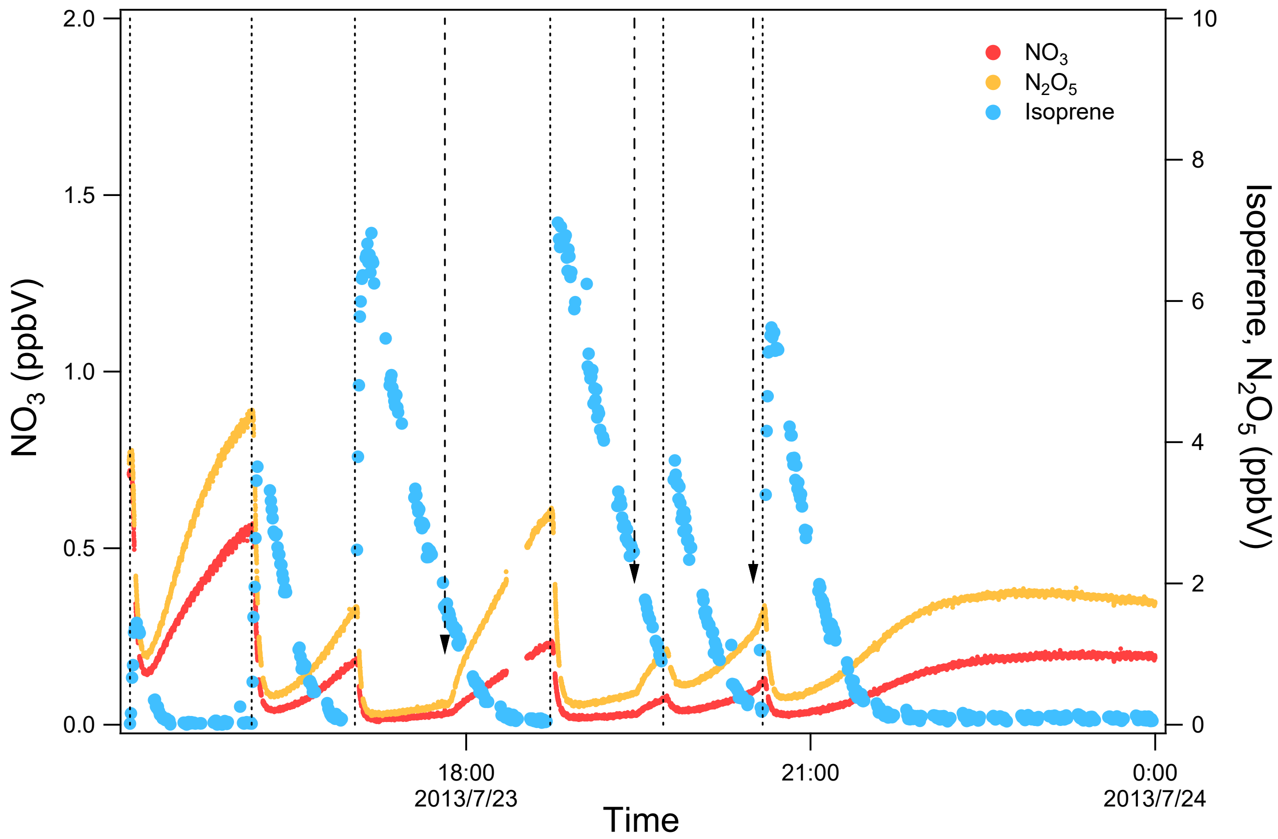

Figure S3. Time series of the of isoprene, NO_3, and N_2O_5 concentration. The dashed lines indicate the time of isoprene additions. The long-dashed arrow indicates the time of NO_2 addition. The dash-dotted arrows indicate the time of O_3 additions.

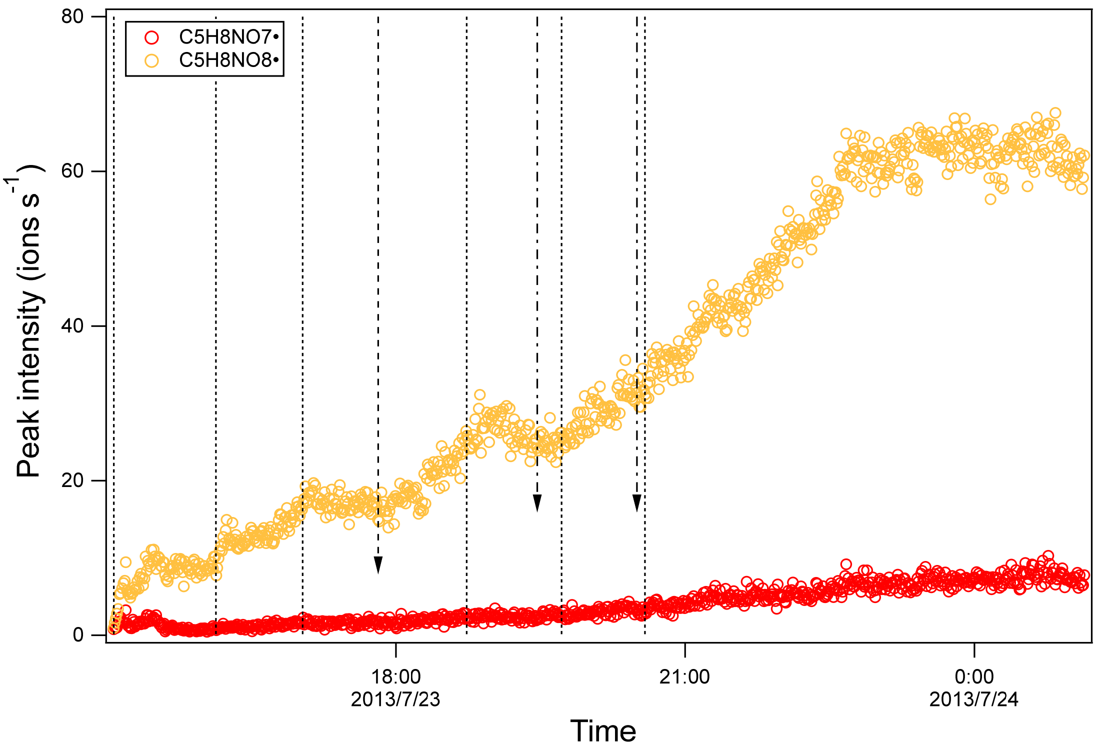

Figure S4. Time series of peak intensity of several HOM monomers of the $C_5H_8NO_n$• series. The dashed lines indicate the time of isoprene additions. The long-dashed arrow indicates the time of NO_2 addition. The dash-dotted arrows indicate the time of O_3 additions.

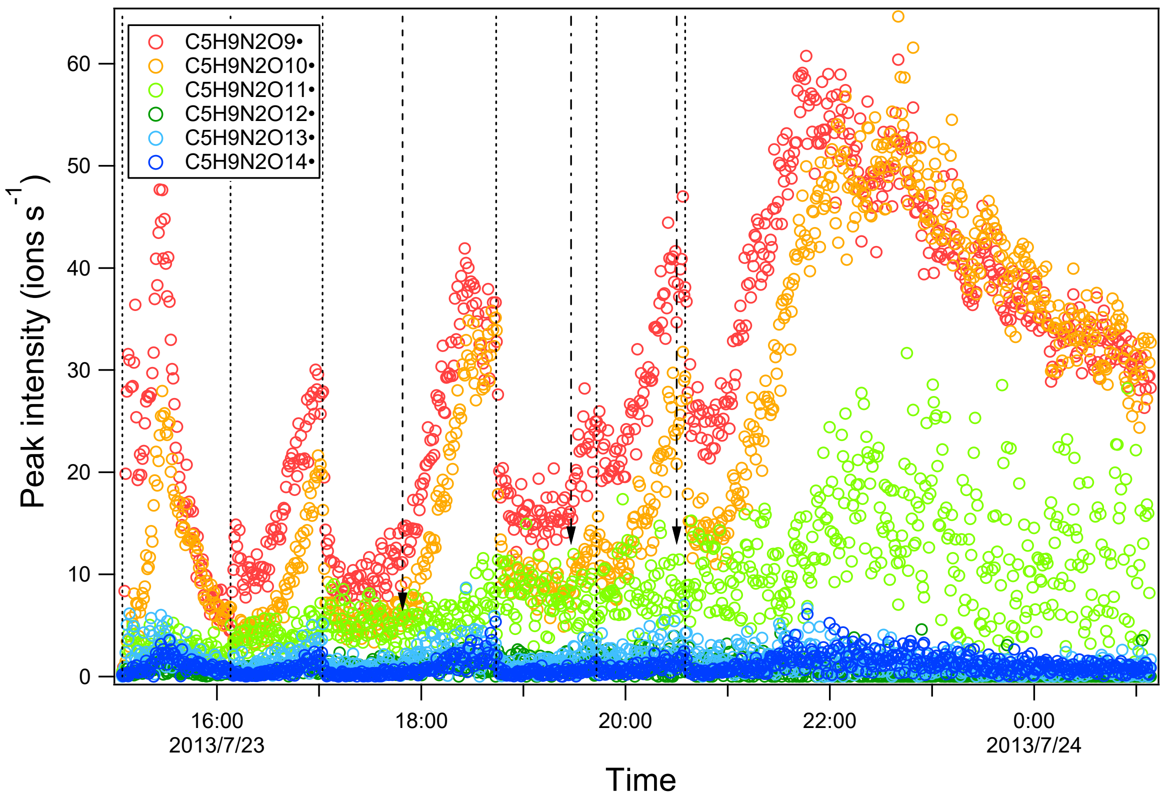

Figure S5. Time series of peak intensity of HOM monomers of the $C_5H_9N_2O_n$• series. The dashed lines indicate the time of isoprene additions. The long-dashed arrow indicates the time of NO_2 addition. The dash-dotted arrows indicate the time of O_3 additions.

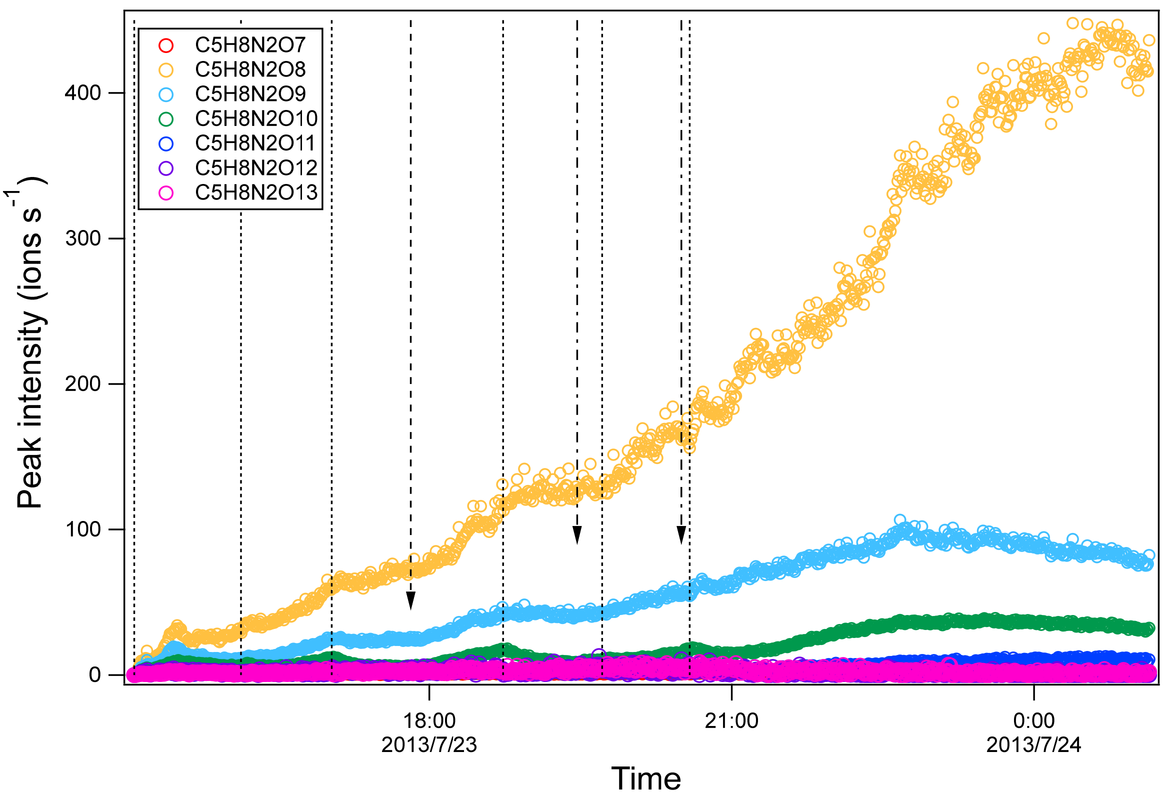

Figure S6. Time series of peak intensity of several HOM monomers of the $C_5H_8N_2O_n$ series (termination products of RO_2 $C_5H_9N_2O_n$). The dashed lines indicate the time of isoprene additions. The long-dashed arrow indicates the time of NO_2 addition. The dash-dotted arrows indicate the time of O_3 additions.

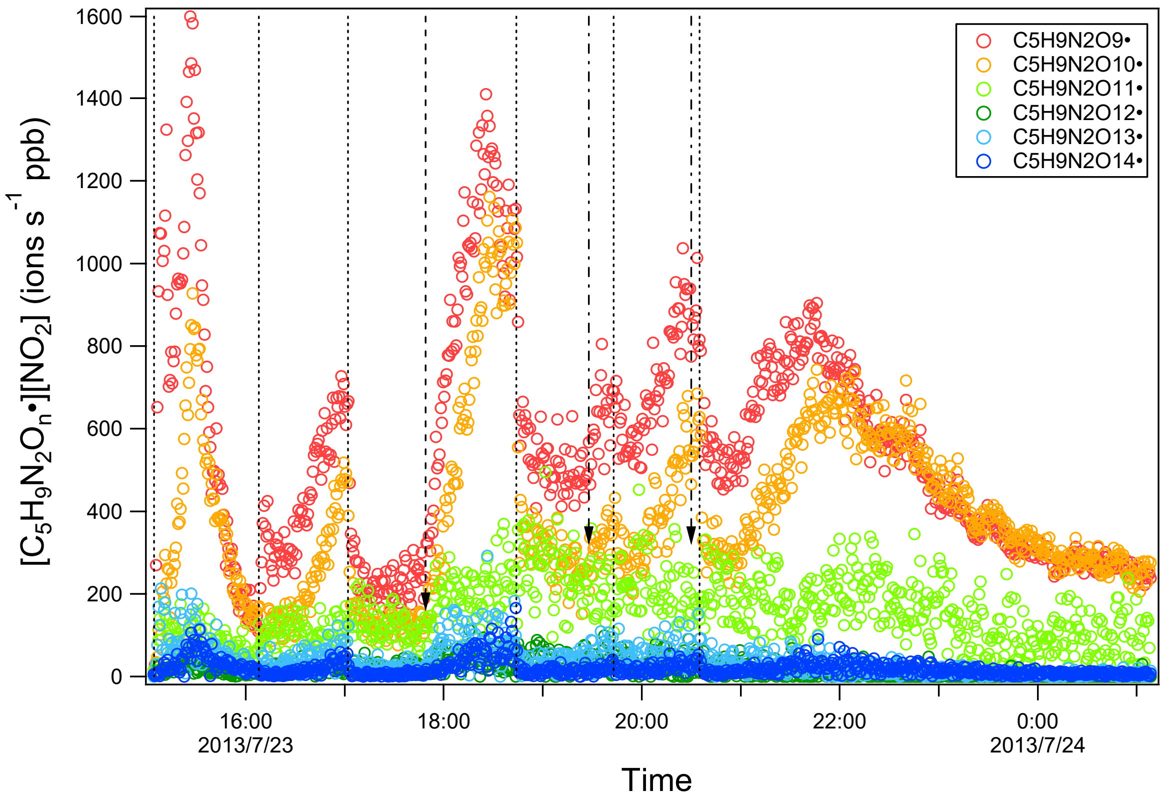

Figure S7. Time series of the product of the peak intensity of $C_5H_9N_2O_n$• and NO_2 concentration. The dashed lines indicate the time of isoprene additions. The long-dashed arrow indicates the time of NO_2 addition. The dash-dotted arrows indicate the time of O_3 additions.

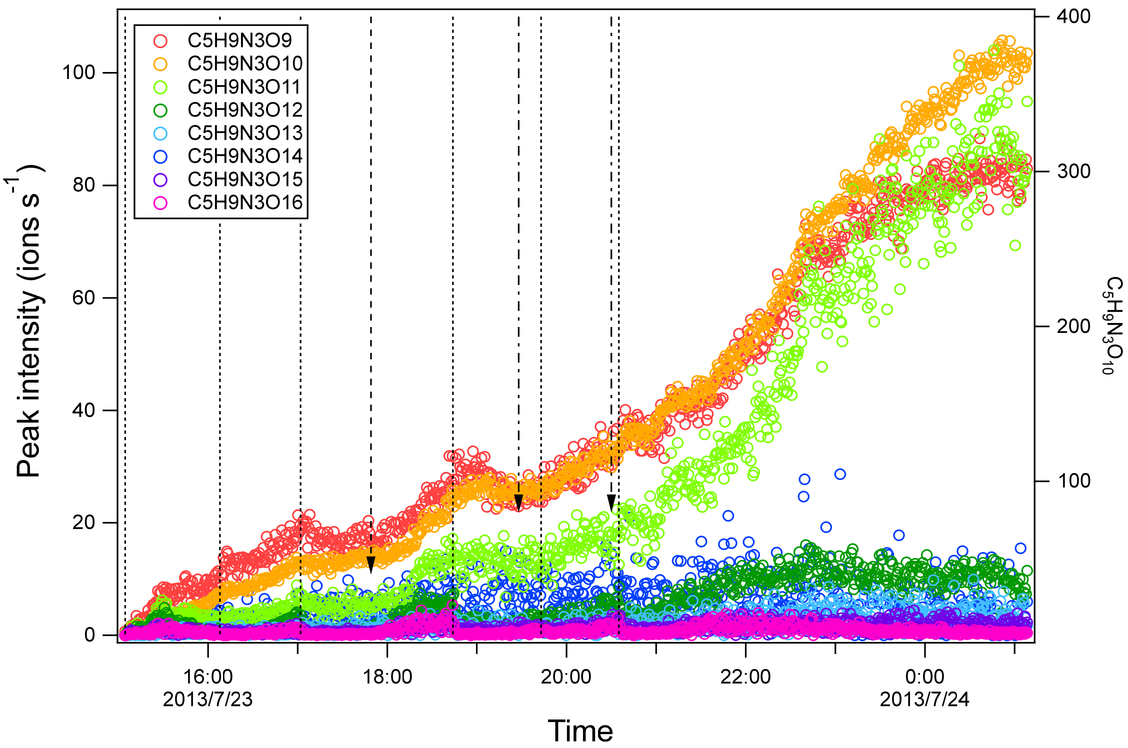

Figure S8. Time series of peak intensity of HOM monomers of the $C_5H_9N_3O_n$ series. The peak intensity of is shown on the left axis except for $C_5H_9N_3O_{10}$. The dashed lines indicate the time of isoprene additions. The long-dashed arrow indicates the time of NO_2 addition. The dash-dotted arrows indicate the time of O_3 additions.

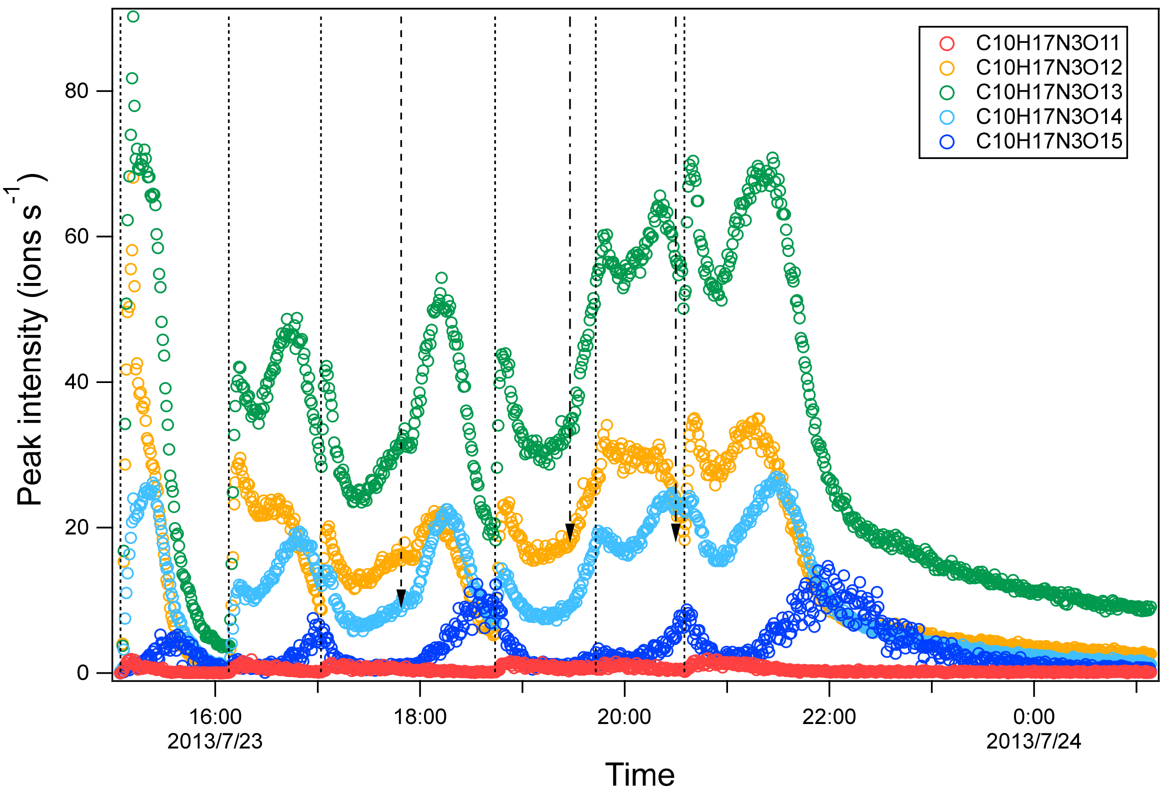

Figure S9. Time series of peak intensity of several HOM dimers of the $C_{10}H_{17}N_3O_n$ series. The dashed lines indicate the time of isoprene additions. The long-dashed arrow indicates the time of NO_2 addition. The dash-dotted arrows indicate the time of O_3 additions.

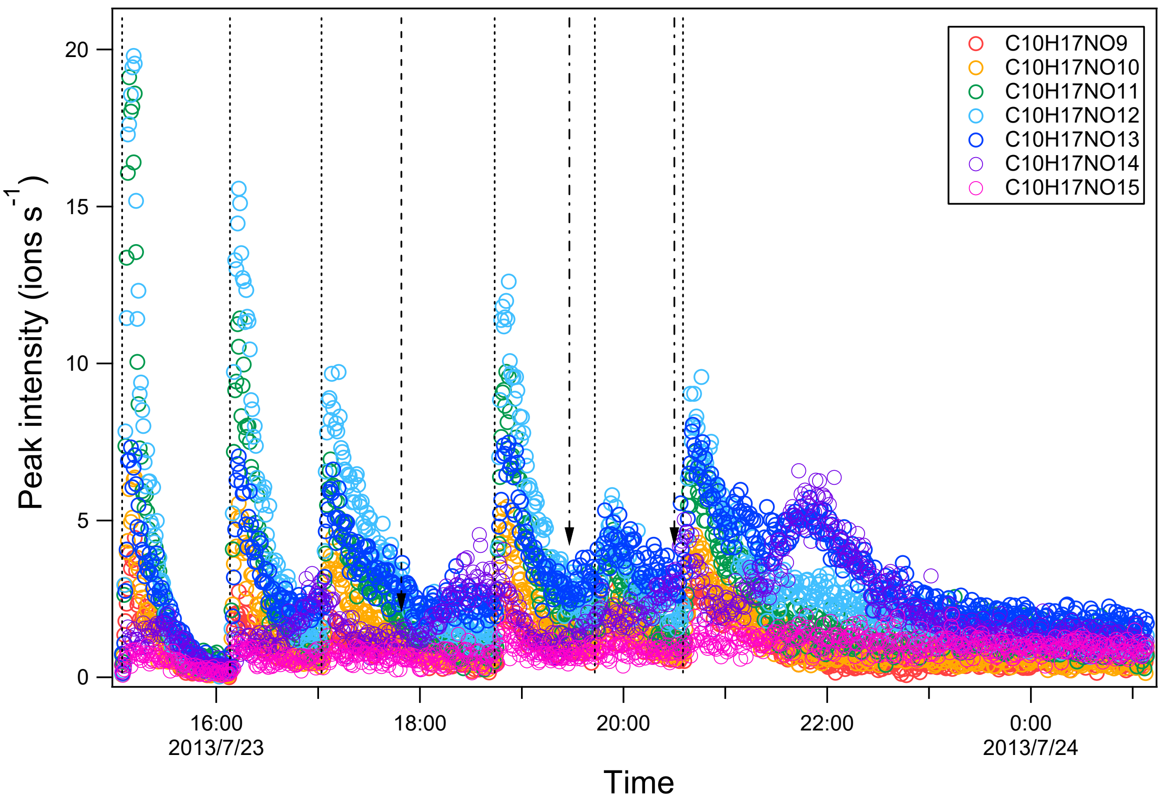

Figure S10. Time series of peak intensity of HOM monomers $C_{10}H_{17}NO_n$ series. The dashed lines indicate the time of isoprene additions. The long-dashed arrow indicates the time of NO_2 addition. The dash-dotted arrows indicate the time of O_3 additions.

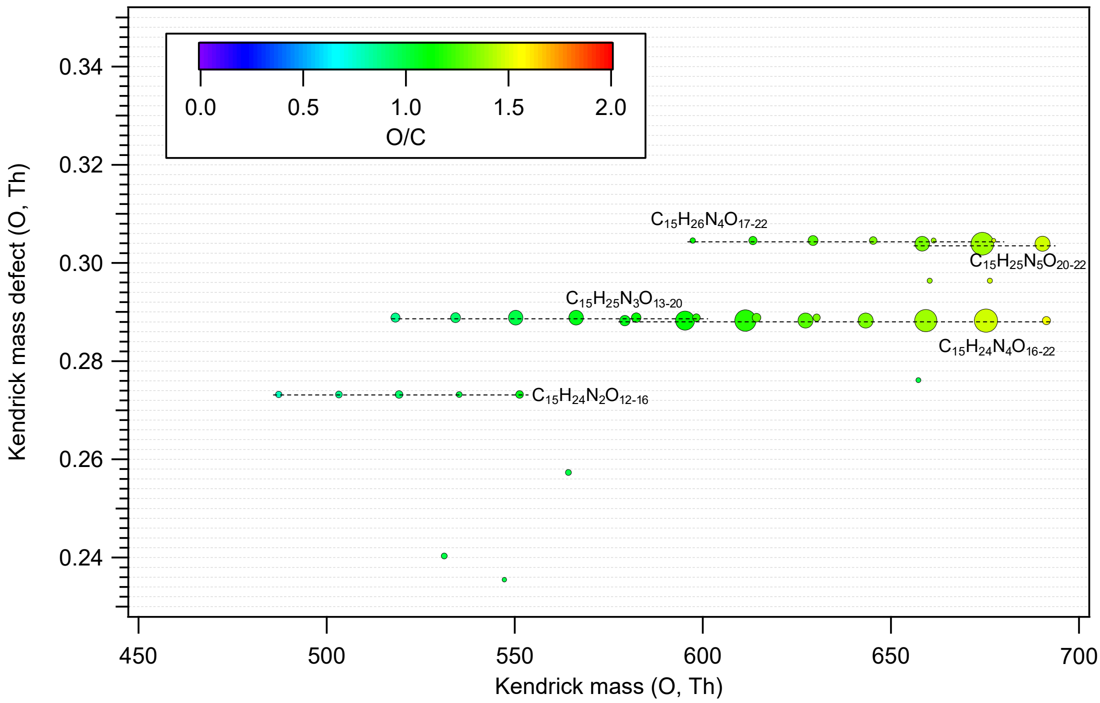

Figure S11. Kendrick mass defect with Kendrick base O of HOM trimers formed in isoprene+NO_3. The area of the circles is set to be proportional to the average peak intensity of each molecular formula during the first isoprene addition period (P1).

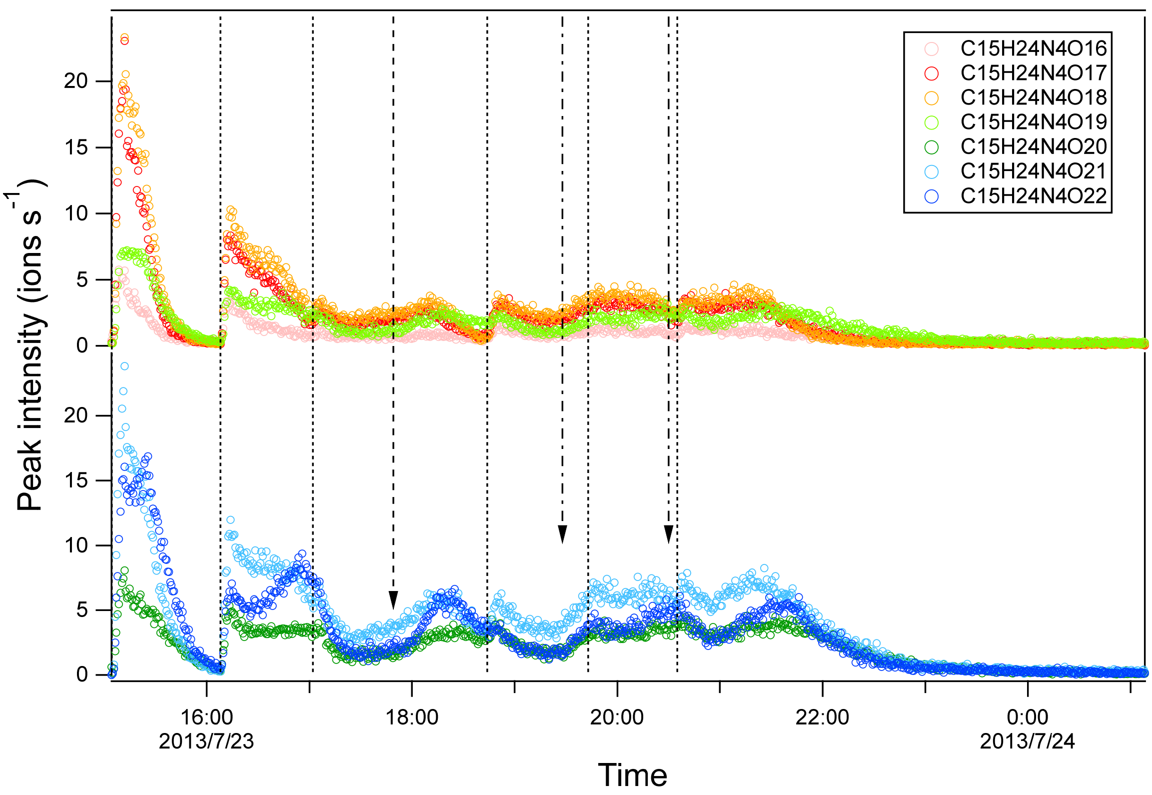

Figure S12. Time series of peak intensity of several HOM dimers of the $C_{15}H_{24}N_4O_n$ series. It is noted that the compounds are plotted in two panels for clarity. The dashed lines indicate the time of isoprene additions. The long-dashed arrow indicates the time of NO_2 addition. The dash-dotted arrows indicate the time of O_3 additions.

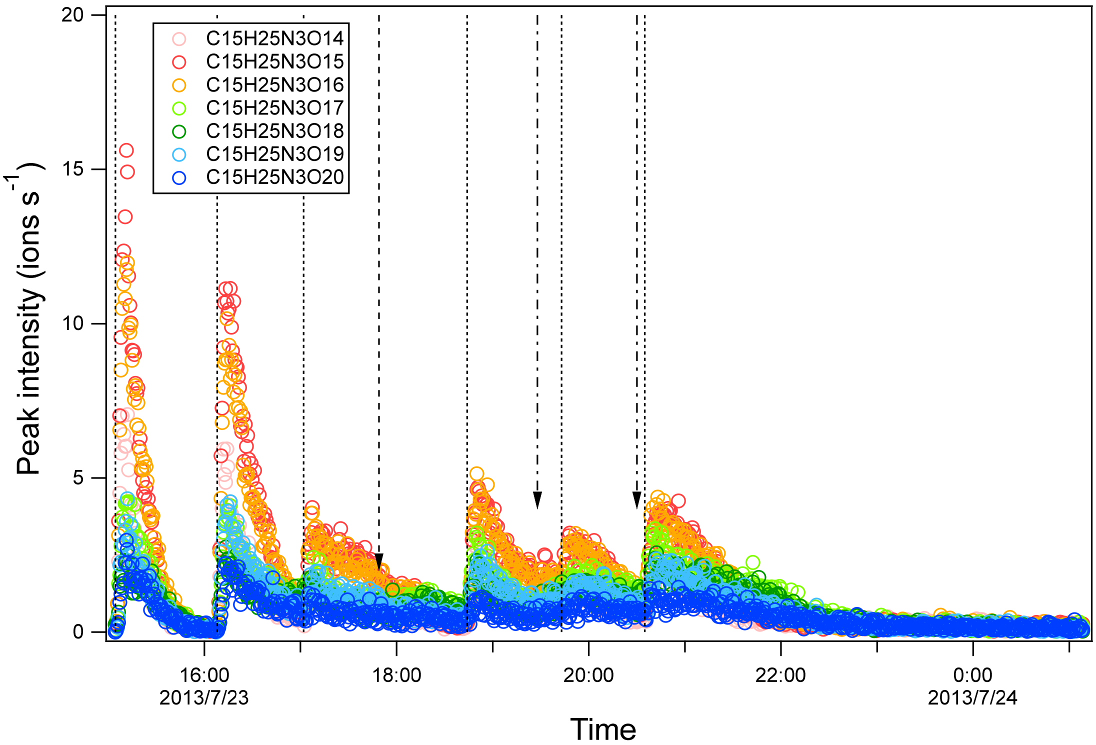

Figure S13. Time series of peak intensity of several HOM dimers of the $C_{15}H_{25}N_3O_n$ series. The dashed lines indicate the time of isoprene additions. The long-dashed arrow indicates the time of NO_2 addition. The dash-dotted arrows indicate the time of O_3 additions.

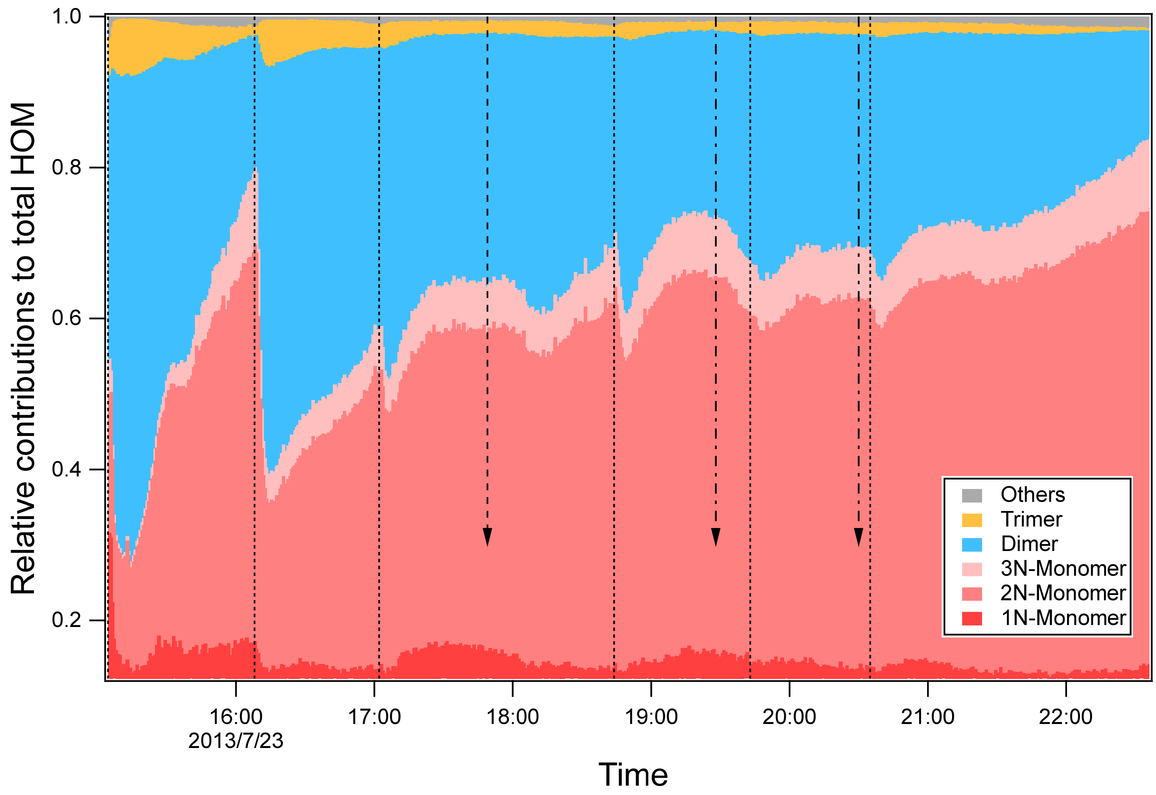

Figure S14. Relative contributions of HOM monomers, dimers, and trimers. Monomer 1-3N refers to the monomers containing 1-3 nitrogen atoms. The dashed lines indicate the time of isoprene additions. The long-dashed arrow indicates the time of NO_2 addition. The dash-dotted arrows indicate the time of O_3 additions.

Table S1. Intensity of HOM monomers $C_5H_8NO_n$ and their corresponding termination products.

Series	**Peroxy radical**	**Carbonyl**	**Hydroxyl**[c]	**Hydroperoxide**[c]	**Carbonyl /Hydroxyl**
m/z	**m**	**m-17**	**m-15**	**m+1**	
M1a	$C_5H_8NO_7$ 257.016 1.5%[a]	$C_5H_7NO_6$ 240.013 4.5%	$C_5H_9NO_6$ 242.028 2.5%	$C_5H_9NO_7$ 258.023 13.9%	1.8
M1b	$C_5H_8NO_8$ 273.010 9.7%	$C_5H_7NO_7$ 256.008 8.1%	$C_5H_9NO_7$ 258.023 13.9%	$C_5H_9NO_8$ 274.018 24.9%[c]	0.6
M1a	$C_5H_8NO_9$ 289.0053 11.9%[b]	$C_5H_7NO_8$ 272.0026 34.0%	$C_5H_9NO_8$ 274.0182 24.9%	$C_5H_9NO_9$ 290.0131 28.5%	1.4
M1b	$C_5H_8NO_{10}$ 305.000 22.2%[b]	$C_5H_7NO_9$ 287.998 8.3%	$C_5H_9NO_9$ 290.013 28.5%	$C_5H_9NO_{10}$ 306.008 5.8%	0.3
M1a	$C_5H_8NO_{11}$ 320.995 2.3%	$C_5H_7NO_{10}$ 303.992 3.0%	$C_5H_9NO_{10}$ 306.008 5.8%	$C_5H_9NO_{11}$ 322.003 2.0%	0.5
M1b	$C_5H_8NO_{12}$ 336.990 1.7%	$C_5H_7NO_{11}$ 319.987 3.0%	$C_5H_9NO_{11}$ 322.003 2.0%	$C_5H_9NO_{12}$ 337.998 2.0%	1.5

[a]: The intensities are average intensity of each peak in MS during the first cycle (C1) normalized to the peak with the maximum intensity ($C_{10}H_{17}N_3O_{13}$).

[b]: These intensities may be subject to higher uncertainties due to the overlap with $C_5H_{10}N_2O_8$ and $C_5H_{10}N_2O_9$.

[c]: The relative contribution of HOM with hydroxyl or hydroperoxide cannot be differentiated and thus the total intensity is listed here.

Table S2. Intensity of HOM monomers $C_5H_9N_2O_n$ and their corresponding termination products.

Series	**Peroxy radical**	**Carbonyl**	**Hydroxyl**	**Hydroperoxide**	**Carbonyl /Hydroxyl**
m/z	**m**	**m-17**	**m-15**	**m+1**	
M2b	$C_5H_9N_2O_8$ 288.021 5.6%[a]	$C_5H_8N_2O_7$ 271.019 1.3%	$C_5H_{10}N_2O_7$ 273.034 0.8%	$C_5H_{10}N_2O_8$ 289.029 99.1%	1.6
M2a	$C_5H_9N_2O_9$ 304.0162 24.9%	$C_5H_8N_2O_8$ 287.0135 57.9%	$C_5H_{10}N_2O_8$ 289.0291 **99.1%**	$C_5H_{10}N_2O_9$ 305.024 82.3%	0.6
M2b	$C_5H_9N_2O_{10}$ 320.011 14.4%	$C_5H_8N_2O_9$ 303.008 29.7%	$C_5H_{10}N_2O_9$ 305.024 82.3%	$C_5H_{10}N_2O_{10}$ 321.019 9.3%	0.4
M2a	$C_5H_9N_2O_{11}$ 336.006 3.3%	$C_5H_8N_2O_{10}$ 319.003 18.3%	$C_5H_{10}N_2O_{10}$ 321.019 9.3%	$C_5H_{10}N_2O_{11}$ 337.014 0.4%	2.0
M2b	$C_5H_9N_2O_{12}$ 352.001 0.7%	$C_5H_8N_2O_{11}$ 334.998 2.5%	$C_5H_{10}N_2O_{11}$ 337.014 0.4%	$C_5H_{10}N_2O_{12}$ 353.009 4.3%	7.1

[a]: The intensities are the average intensities of each peak in MS during the first cycle (C1) normalized to the peak with the maximum intensity ($C_{10}H_{17}N_3O_{13}$).

[b]: The relative contribution of HOM with hydroxyl or hydroperoxide cannot be differentiated and thus the total intensity is listed here.

Table S3. Summary of the major HOM products in the reaction of isoprene with NO_3

Molecular Formula	**m/Q**	**HOM series[a]**
C5H7NO5	224.017	Monomer 1
C5H7NO6	240.012	Monomer 1
C5H8NO10	241.020	Monomer 1
C5H9NO6	242.028	Monomer 1
C5H7NO7	256.007	Monomer 1
C5H8NO6	257.015	Monomer 1
C5H9NO7	258.023	Monomer 1
C5H11NO7	260.038	Monomer 4
C5H7NO8	272.002	Monomer 1
C5H8NO11	273.010	Monomer 1
C5H9NO8	274.018	Monomer 1
C5H10NO8	275.025	Monomer 4
C5H11NO8	276.033	Monomer 4
C5H8N2O8	287.013	Monomer 2
C5H7NO9	287.997	Monomer 1
C5H8NO7	289.005	Monomer 1
C5H10N2O8	289.029	Monomer 2
C5H9NO9	290.013	Monomer 1
C5H10NO9	291.020	Monomer 4
C5H11NO9	292.028	Monomer 4
C5H9N3O10	302.024	Monomer 2
C5H8N2O9	303.008	Monomer 2
C5H7NO10	303.992	Monomer 1
C5H9N2O9	304.016	Monomer 2
C5H8NO12	305.000	Monomer 1
C5H10N2O9	305.023	Monomer 2
C5H9NO10	306.007	Monomer 1
C5H11NO10	308.023	Monomer 4
C5H9N3O11	318.019	Monomer 2
C5H9N3O9	318.019	Monomer 2
C5H8N2O10	319.003	Monomer 2
C5H7NO11	319.987	Monomer 1
C5H9N2O10	320.011	Monomer 2
C5H8NO8	320.995	Monomer 1
C5H10N2O10	321.018	Monomer 2
C5H9NO11	322.002	Monomer 1
C5H11NO11	324.018	Monomer 4
C5H9N3O12	334.014	Monomer 2
C5H8N2O11	334.998	Monomer 2
C5H7NO12	335.982	Monomer 1
C5H9N2O11	336.005	Monomer 2
C5H10N2O11	337.013	Monomer 2
C5H9NO12	337.997	Monomer 1
C5H9N3O13	350.009	Monomer 2
C5H9N2O12	352.000	Monomer 2

C5H8NO9	352.984	Monomer 1
C5H10N2O12	353.008	Monomer 2
C5H9N3O14	366.003	Monomer 2
C5H9N2O13	367.995	Monomer 2
C5H10N2O13	369.003	Monomer 2
C5H9N3O15	381.998	Monomer 2
C5H9N2O14	383.990	Monomer 2
C10H16N2O10	387.065	Dimer 1
C10H18N2O10	389.081	Dimer 4
C10H16N2O11	403.060	Dimer 1
C10H17N2O11	404.069	Dimer R2
C10H18N2O11	405.076	Dimer 4
C10H17N3O11	418.071	Dimer 2
C10H16N2O12	419.055	Dimer 1
C10H17N2O12	420.064	Dimer R2
C10H18N2O12	421.071	Dimer 4
C10H16N3O12	433.059	Dimer R1
C10H17N3O12	434.066	Dimer 2
C10H16N2O13	435.050	Dimer 1
C10H18N2O13	437.066	Dimer 4
C10H15N3O13	448.045	Dimer 5
C10H16N3O13	449.054	Dimer R1
C10H17N3O13	450.061	Dimer 2
C10H16N2O14	451.045	Dimer 1
C10H18N2O14	453.061	Dimer 4
C10H15N3O14	464.040	Dimer 5
C10H16N3O14	465.049	Dimer R1
C10H17N3O14	466.056	Dimer 2
C10H16N2O15	467.040	Dimer 1
C10H18N2O15	469.056	Dimer 4
C10H15N3O15	480.035	Dimer 5
C10H16N3O15	481.044	Dimer R1
C10H17N3O15	482.051	Dimer 2
C10H16N2O16	483.035	Dimer 1
C10H18N2O16	485.050	Dimer 4
C10H15N3O16	496.030	Dimer 5
C10H16N3O16	497.038	Dimer R1
C10H18N4O15	497.062	Dimer 3
C10H17N3O16	498.046	Dimer 2
C10H16N2O17	499.030	Dimer 1
C15H25N3O12	502.129	Trimer 3
C10H15N3O17	512.025	Dimer 5
C10H17N4O16	512.049	Dimer R3
C10H18N4O16	513.057	Dimer 3
C10H17N3O17	514.041	Dimer 2
C15H25N3O13	518.124	Trimer 3
C10H17N4O17	528.044	Dimer R3
C10H18N4O17	529.052	Dimer 3

C10H17N3O18	530.036	Dimer 2
C15H25N3O14	534.119	Trimer 3
C10H17N4O18	544.039	Dimer R3
C10H18N4O18	545.046	Dimer 3
C10H17N3O19	546.031	Dimer 2
C15H25N3O15	550.114	Trimer 3
C15H25N3O16	566.109	Trimer 3
C15H25N3O17	582.104	Trimer 3
C15H24N4O17	595.099	Trimer 1
C15H26N4O17	597.115	Trimer 4
C15H25N3O18	598.099	Trimer 3
C15H24N4O18	611.094	Trimer 1
C15H26N4O18	613.110	Trimer 4
C15H25N3O19	614.094	Trimer 3
C15H24N4O19	627.089	Trimer 1
C15H26N4O19	629.105	Trimer 4
C15H25N3O20	630.089	Trimer 3
C15H24N4O20	643.084	Trimer 1
C15H26N4O20	645.099	Trimer 4
C15H25N5O20	658.095	Trimer 2
C15H24N4O21	659.079	Trimer 1
C15H26N4O21	661.094	Trimer 4
C15H25N5O21	674.090	Trimer 2
C15H24N4O22	675.074	Trimer 1
C15H25N5O22	690.085	Trimer 2

[a]: The numbering of HOM series is referred to the main text.